

Investigation of the Sensitivity Parameters to Automatic Cavitation in Hydro turbines of the Sefid Rood Dam Considering Useful Life

Ramtin Sobhkhiz Foumani¹, Alireza Mardookhpour², Sara Kohansal³

1- M.Scof Civil Engineering Department, Islamic Azad University of Lahijan, Lahijan, Iran

2- Assistant Professor of Civil Engineering Department, Islamic Azad University of Lahijan, Lahijan, Iran

3- M.Scof Civil Engineering Department, Islamic Azad University of Lahijan, Lahijan, Iran

Corresponding Author's E-mail: Sobhkhizarman@yahoo.co.uk

Abstract

In this research, the evaluation of cavitation threshold detection and the automation of the detection process with regard to the Remaining Useful Life (RUL) of the Sefidrood power plant turbine, has been studied. The input of generated model by MATLAB program includes data driven from Kaplan hydro turbine located on Tarik hydro power plant. The proposed model is based on 61 features resulting from 6 cavitation sensitivity parameters and 17 operational conditions. For training in MATLAB program, 12 individual data sets and 4095 unique combinations were created and 408 data were selected for examination. The training data combined with sensor rating and cavitation sensitivity feature were employed to predict the cavitation and the best training data set with 98% accuracy. The results showed that the use of a fully automated process for sensitivity determination and cavitation classification was more suitable than the use of a process based on manually selected thresholds. Furthermore, considering the operational conditions and RUL, the automation of determination of cavitation threshold without human intervention was much more accurate.

Keywords: Hydro power plant, Cavitation detection, Remaining useful life (RUL), Kaplan turbine, MATLAB program.

Introduction

The hydroelectric power makes up 98.8% of the national electricity generation and 13.8% of the total electricity produced in Iran. While hydroelectricity accounts for about 19% of the world's total electrical energy. Cavitation damage to hydro turbine blades is an expensive problem that reduces power generation and turbine life. Bajic et al. (2003) compared the sensors, the location of the sensors or the cavitation sensitivity parameters (CSP). Francois (2012) Showed that no studies have been published to estimate the hydro turbine erosion rate. Data from the hydro turbine blade inspections were collected in an attempt to provide a model of erosion rates based on the Wolff et al. (2005) inspection reports, but their collected data was not enough. Scaler et al. (2014) and Cencic et al. (2014) Suggested that cavitation detection features and their identification methods may be used to estimate the erosion or prediction of remaining useful life, but have so far failed to implement it in a hydro turbine at the hydroelectric plant. There appears to be no general study on the prediction of hydro turbine erosion or the remaining useful life prediction method. In addition, no research has been done on the selection of the cavitation detection features. Up to now, nobody has tried to identify the features of the cavitation detection in a suitable iterative approach for hydro-turbines. Despite the advances in the design of water turbines, the damage caused by cavitation is one of the main reasons for the failure of the turbine (Dorji and Ghomashchi, 2014). This also highlights the importance of developing better methods for detecting erosion cavitation in water turbines. The aim of this research is to attempt to develop a data-based model for the detection of automatic

cavitation and estimate the erosion rate of cavitation for a long time in a case study based on data obtained from the of the SefidRood dam turbine considering remaining useful life (RUL).

2. Methods and materials

Study area: The Tarik hydroelectric power plant of Sefidrood dam is located at longitude of 36° 58' and latitude of 49° 35', with a distance of approximately 35 km downstream of the Sefidrood storage dam in the Gilan province. The dark diversion dam is considered to be the first bulb turbine power plant in the country and since this type of turbine is used for low water level and high discharge, it can be used in most small dams and less mountainous and watery areas, such as the northern areas of the country. Figure 1 shows a view of the Sefidrood dam. The general specifications of the power plant equipment include two turbine generator units of the Kaplan type. The case study is investigation of real cavitation over Kaplan PIT x1500 KW turbine which have cavitation erosion over leading edge of blades.

Table1. The calculations used for the values of the cavitation sensitivity parameter features.

| Calculation | Formula |
|---------------------|---|
| Average square root | $f_{rms} = \sqrt{\frac{\sum_{n=1}^N X_n^2}{N}}$ |
| Peak | $f_{peak} = \max(x)$ |
| Peak factor | $f_{CF} = \frac{f_{peak}}{f_{rms}}$ |
| Kurtosis | $f_{kurt} = \frac{\frac{1}{N} \sum_{n=0}^N [x_n - \bar{\mu}_x]^4}{\left(\frac{1}{N} \sum_{n=0}^N [x_n - \bar{\mu}_x]^2\right)^2}$ |

f_{rms} is average square root and f_{peak} is maximum peak domain of a periodic quantity that is calculated respect to its zero value and f_{CF} is the ratio of peak to the effective value of two periodic quantity and f_{kurt} is sharpness of the peak of the curve, which shows the extent and frequency of the mean and is the peak level in a statistical graph.

Data have been prepared in 3 steps. (1) cavitation sensitivity parameter (CSP) has been defined, data were collected from the cavitation analysis, including sensor types, location of sensors and operating conditions, and the values were calculated for entering the developed matrix. (2) Cavitation sensitivity parameters were organized in columns of a characteristic matrix. (3) The matrix columns were normalized using z-score transformation. The new normalized value has no unit and the size of the standard deviation is the average of the data. Proposed method was shown with 61 features derived from 6 unique cavitation sensitivity parameters and 17 unique operating conditions. The analysis of the main component in the correlation matrix F was done to obtain P (Jolliffe, 2002). F using P to construct a new representation of the main data turned to Y and each score vector of the main component in Y was plotted to observe a variance for each main component in accordance with equation (1). The conversion was calculated as follows:

$$P * F = Y \quad (1)$$

To select the cavitation detection feature, the main components that are not dependent on the cavitation erosion must be eliminated. Bajic (2002) developed a multidimensional technique that is effective for all types of hydro

turbines. Investigations of Rus et al. (2007) and Escaler et al. (2014) using the first signals of the band-pass filter sensor, showed a good cavitation detection. Evaluation of the mean root mean of sensor signals is a method widely used to detect cavitation detection. Generally, the calculated RMS of raw sensor signals is sensitive to disruptive events. Cencic et al. (2014) evaluated five frequency ranges for cavitation response, and finally, a specific frequency range was shown as the best cavitation sensitive range.

2.1 Cavitation intensity and intensity measurement

The cavitation intensity can be measured through vibration sensors, acoustic emission, and the duration of exposure to cavitation to estimate cavitation degradation and the remaining useful life. Measurement scale of cavitation sensitivity parameter is dependent on the sensor type and the measured value is affected by the sensor location (Dular et al., 2006). Accumulated cavitation intensity at total data sets, I_{total} , was calculated from Eq. (2).

$$I_{total} = \sum (X_{MD-cavitation})(t_{blok}) \quad (2)$$

$X_{MD-cavitation}$ is Mahalanobis distance from every parameter of cavitation sensitivity identified by the classification

as a cavitation class and t_{blok} is the time length of the block used to create the cavitation sensitivity parameter.

The precision of the cavitation classification has been calculated in four ways: 1) A simple threshold rank classification and manual threshold selection. 2) Simple threshold classification and an unattended learning algorithm; 3) A supervised learning algorithm (supporting vector machines) and training data that are manually labeled. 4) A supervised learning algorithm and training data that is labeled with a unsupervised learning algorithm (K-Means) using the MATLAB program.

2.2 Features selection for cavitation detection

The purpose of this process is to select the best long-term cavitation detection feature for a unique hydroturbine. The correlation coefficient between the scores of the main component and the normal attribute was calculated. To compare the correlation coefficients, it can be referred to Holick (2013). In this research and based on experience-based law, a very high degree of dependence on the main component scores related to cavitation erosion was selected and items with an absolute value of less than 0.9 were removed. The standard deviation for each feature under hydroturbine operating conditions was evaluated with minimal cavitation ($S_{CSP-min}$) and maximum cavitation ($S_{CSP-max}$) and dispersion of features was evaluated. To remove additional features and thresholds Eq. (3) has been used.

$$\begin{aligned} \text{Threshold 1} &= 2 \times S_{CSP - min} \\ \text{Threshold 2} &= 2 \times S_{CSP - max} \end{aligned} \quad (3)$$

The remaining features were ranked based on a combination of standard deviations and according to Eq. (4) to determine the best features for long-term monitoring.

$$S_{CSP \text{ compound}} = S_{CSP - min} + S_{CSP - max} \quad (4)$$

The best features of cavitation have the lowest values. Finally, the features were selected based on the final subjective evaluation and based on practical considerations for long-term cavitation detection. The low ramp

data was collected and divided into 1 block of seconds and direct current (frequency Zero) was eliminated in each block and the Fourier discrete conversion of each block and sample variance of each frequency value were calculated. The output for a frequency plot compared to the range, called the frequency spectrum.

3. Results and discussions

In the first step of the feature selection process, 6 value of the cavitation sensitivity parameter for each sensor was calculated in which the high frequency data and 5 values for which the mean frequency data were collected. The cavitation feature matrix was created by computing the values of the cavitation sensitivity parameter mentioned in Table 1 for three acoustic emission sensors, three accelerometers, four proximity probes and a pressure transducer in a cavitation analysis with 61 general characteristics. 32 value of the cavitation sensitivity parameter for each of the 17 operating modes was obtained and, thus, 544 the value of the cavitation sensitivity parameter was obtained for each feature. Feature naming is a combination of the abbreviation of the sensor type and the parameter number of the cavitation sensitivity.

Table 1. Details of the cavitation sensitivity parameter for each type of sensor

| Sensor type | Cavitation sensitivity parameter |
|---------------------------|--|
| Accelerometers | <ol style="list-style-type: none"> 1. Average square root domain 1000 to 20,000 Hz 2. Average square root domain 20,000 to 30,000 Hz 3. Average square root domain 30,000 to 100,000 Hz 4. Peak domain 1000 to 20,000 Hz 5. Peak coefficient 10,000 to 20,000 Hz 6. Kurtosis 1000 to 20,000 Hz |
| Acoustic emission sensors | <ol style="list-style-type: none"> 1. Average square root domain 1000 to 4000 Hz 2. Average square root domain 50,000 to 400,000 Hz 3. Average square root domain 1000 to 50,000 Hz 4. Peak domain 1000 to 4000 Hz 5. Peak coefficient 1000 to 400,000 Hz 6. Kurtosis 1000 to 400,000 Hz |
| Proximity probes | <ol style="list-style-type: none"> 1. Average square root domain 40 to 1000 Hz 2. Average square root domain 1 to 40 Hz 3. Peak domain 40 to 1000 Hz 4. Peak coefficient 40 to 1000 Hz 5. Kurtosis 40 to 1000 Hz |
| Pressure transducer | <ol style="list-style-type: none"> 1. Average square root domain 40 to 1000 Hz 2. Average square root domain 1 to 40 Hz 3. Peak domain 40 to 1000 Hz 4. Peak coefficient 40 to 1000 Hz 5. Kurtosis 40 to 1000 Hz |

The normalization of the feature matrix and the analysis of the main component was done using MATLAB software and resulted in the matrix of the scores of the original component Y.

3.1. Classification test results

Taking into account 17 unique speeds and 24 seconds of data for each flow rate, 408 blocks of vibration data were used to generate test data. The simple classifier algorithms and the supporting vector machine have been applied to the test data and the results of the group predictions were compared with the appropriate group labels for accuracy determination. Equation (5) was used to calculate the accuracy.

Accuracy = a group of label/total

(5)

The accumulated cavitation intensity in the entire data set is shown in Table 2. For supporting vector machine results, the probe/cavitation sensitivity parameters pairs were summed up with the first proximity probe, for example, a training set created with data collected from the proximity probe 1 from the frequency range 1 is used to calculate the cavitation sensitivity parameter, which briefly represented as "PP1-CSP".

Table 2. Classifier test results for univariate threshold.

| Classifier | Training and test sets | Accuracy results | Total |
|---|--|------------------|-------|
| Simple, with the manual threshold selected | Proximity probe 1 | 95.3 | 2457 |
| | Proximity probe 2 | 95.3 | 2473 |
| | Proximity probe 3 | 93.6 | 2696 |
| | Proximity probe 4 | 92.2 | 2395 |
| Simple, with the Kmeans threshold selected | Proximity probe 1 | 91.2 | 2433 |
| | Proximity probe 2 | 94.6 | 2473 |
| | Proximity probe 3 | 89.0 | 2661 |
| | Proximity probe 4 | 85.1 | 2395 |
| Supporting vector machine, with the manual threshold selected | PP2-CSP1, PP2-CSP3, PP3-CSP3, PP2-CSP2 | 95.6 | 2446 |
| | PP2-CSP1, PP2-CSP3, PP3-CSP3, PP2-CSP2, PP3-CSP2 | 95.3 | 2433 |
| | PP1-CSP3, PP2-CSP3, PP3-CSP3, PP2-PP1-CSP2 CSP2 | 95.1 | 2520 |
| | PP3-CSP1, PP4-CSP1, PP1-CSP3, PP4-CSP3, PP3-CSP2 | 99.0 | 2638 |
| Supporting vector machine, with the manual threshold selected | PP3-CSP1, PP4-CSP1, PP1-CSP3, PP2-CSP3, PP4-CSP3, PP4-CSP2 | 98.7 | 2633 |
| | PP3-CSP1, PP4-CSP1, PP1-CSP3, PP2-CSP3, PP4-CSP3, PP1-CSP2, PP4-CSP2 | 98.7 | 2640 |
| | PP3-CSP1, PP4-CSP1, PP1-CSP3 | 98.5 | 2625 |

The accuracy results of the second to seventh classifier based on the multivariate thresholds are shown in Table 2. The graphical representation of the correct classification labels for the test data is shown in Figure 1 by manual method and in Figure 2 by the k-means clustering method and in Figures 3 and 4 by a supporting vector machine classification.

Table 5. Classifier test results for multivariate threshold.

| Classifier | Training and test sets | Accuracy results | Total |
|---|-----------------------------------|------------------|-------|
| Non-linear supporting vector machine with a multivariate threshold manually selected | CSP2, CSP3, 2nd order | 94.1 | 2711 |
| | CSP1, CSP2, CSP3, 3rd order | 94.4 | 2720 |
| | CSP1, CSP2, CSP3, 4th order | 96.8 | 2829 |
| | CSP1, CSP2, CSP3, 5th order | 97.8 | 2866 |
| | CSP1, CSP2, CSP3, 6th order | 97.3 | 2833 |
| | CSP1, CSP2, CSP3, 7th order | 96.8 | 2798 |
| Non-linear supporting vector machine with a multivariate threshold by K-mean method | CSP3, 3rd order | 93.6 | 2777 |
| | CSP3, 3rd order | 94.0 | 2696 |
| | CSP1, CSP2, CSP3, 4th order | 95.1 | 2916 |
| | CSP1, CSP2, CSP3, 5th order | 97.5 | 2891 |
| | CSP1, CSP2, CSP3, 6th order CSP1, | 97.3 | 2891 |
| | CSP2, CSP3, 7th order | 96.8 | 2951 |
| Simple, with a multivariate threshold selected manually, with a multivariate threshold selected in the K-mean method (same results) | | | |
| CSP3 | | 94.1 | 2711 |

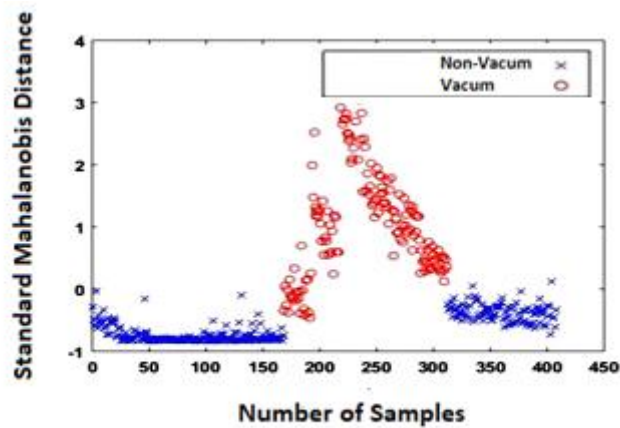


Figure 1. cavitation data with correct label using manual method.

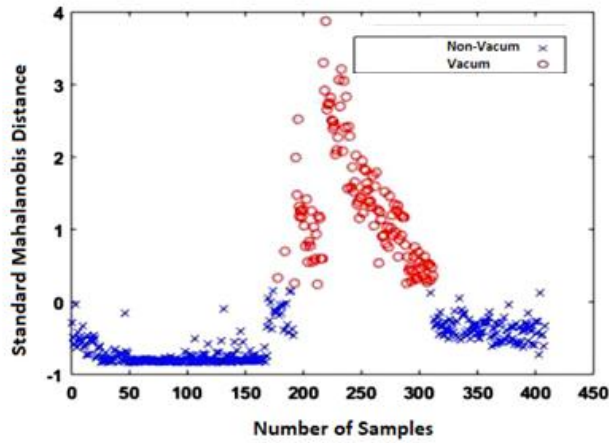


Figure 2. cavitation data with correct label using k-mean clustering method.

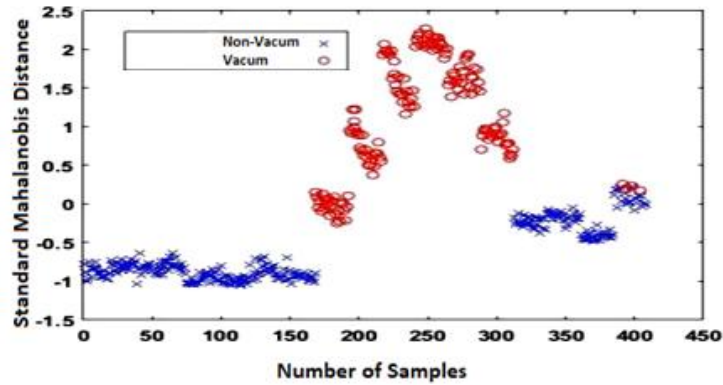


Figure 3. cavitation data labeled with a manually selected supporting vector machine model, univariate threshold and training set 'PP4-CSP3', PP1-CSP3', PP4-CSP1', PP3-CSP1, PP3-CSP2.

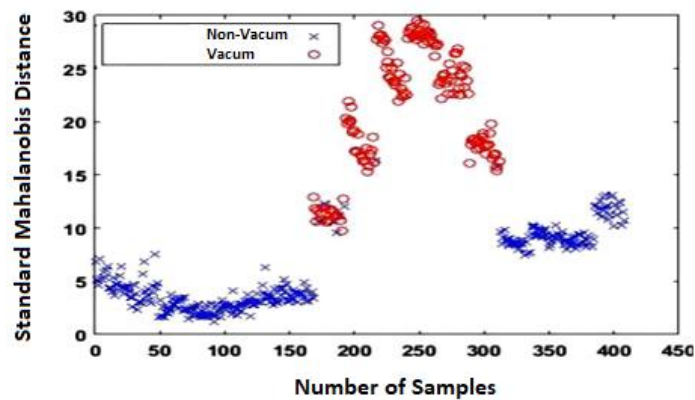


Figure 4. cavitation data labeled with supporting vector machine (5th order) model, multivariate threshold using k-mean clustering.

4. Conclusion

The process of selecting the features described in this study was based on the data of the cavitation studies in a Kaplan hydroturbine. CSP3 was superior in several results, and the precision of this compound is more than 98% in the prediction of cavitation. From more explicit sources of adding data, choosing a polynomial order is for nonlinear thresholds. The most precise nonlinear thresholds were obtained using a fifth-order polynomial. In manually selected based thresholds, the precision of 95% was obtained and in the fully automated process, which was used using K-Means clustering and supporting vector machine for detecting cavitation, a precision of 98% was obtained, which considering the time needed for analysis shows the usefulness of the machine learning framework in comparison with the manual method. This method is used to identify the cavitation sensitivity parameter, to automate the training process and to classify correctly and also be used to determine the threshold that is easily adapted to the changing conditions of the hydroturbine, with minimal disruption of power production and without human intervention.

5. Resources

- [1] Bajc, B. (2002). "Multidimensional diagnostics of turbine cavitation", *Journal of Fluids Engineering*, 124(4), pp. 943-950.
- [2] Bajic, B., Korto, C. (2003). "Methods for vibroacoustic diagnostics of turbine cavitation Méthodes pour le diagnostic vibro-acoustique de la cavitation de turbine", *Journal of Hydraulic Research*, 3(41), pp. 87-96.
- [3] Cencic, T., Hocevar, M., Sirok, B. (2014). "Study of erosive cavitation detection in pump mode of pump-storage hydropower plant prototype", *ASME, Journal of Fluids Engineering*, 136(5), pp.1-11.
- [4] Dorji, U., Ghomashchi, R. (2014). Hydro turbine failure mechanism: *An overview, Engineering Failure Analysis*, (44), pp. 136-147.
- [5] Jolliffe, T. (2002). *Principal Component Analysis, Second Edition*, Encyclopedia of Statistics in Behavioral Science, University of Aberdeen, UK
- [6] Rus, T., Dular. M., Marko, H. (2007). "An investigation of relationship between acoustic emission, vibration, noise and cavitation structures on Kaplan turbine", *Journal of Fluids Engineering*, 129(9), pp. 1112-1122.
- [7] Wolff, P. (2013). "Evaluation of results from acoustic emission-based cavitation monitor", Grand Coulee Project, Technical report, Hydro Performance Processes, Incpp. 89-99.
- [8] Dular, M. Stofefel, B., Sirok, B. (2006). "Development of cavitation erosion model", *Wear*, 261(5-6), pp. 642-655.
- [9] Escaler, X., Viktor, E. Franke, H. (2014). "Detection of draft tube surge and erosive blade cavitation in a full-scale Francis turbine", *Journal of Fluids Engineering*, 137(1), pp. 103-115.
- [10] Francois, L. (2012). "Vibratory detection system of cavitation erosion: Historic and algorithm validation", *Proceedings of the 8th international symposium on cavitation*, pp. 44-65, Singapore.
- [11] Holick, M. (2013). *Introduction to probability and statistics for engineers*, University of California, Berkeley.